

Align-DETR: Improving DETR with Simple IoU-aware BCE loss

Zhi Cai^{1,2*} Songtao Liu² Guodong Wang¹ Zheng Ge²
 Zeming Li² Xiangyu Zhang² Di Huang¹
¹Beihang University
²MEGVII Technology

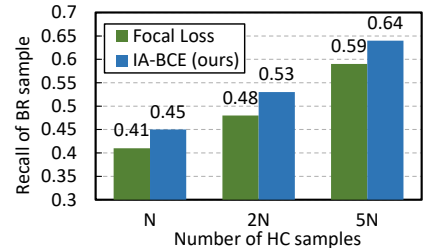
Abstract

DETR has set up a simple end-to-end pipeline for object detection by formulating this task as a set prediction problem, showing promising potential. However, despite the significant progress in improving DETR, this paper identifies a problem of misalignment in the output distribution, which prevents the best-regressed samples from being assigned with high confidence, hindering the model’s accuracy. We propose a metric, recall of best-regressed samples, to quantitatively evaluate the misalignment problem. Observing its importance, we propose a novel Align-DETR that incorporates a localization precision aware classification loss in optimization. The proposed loss, IA-BCE, guides the training of DETR to build a strong correlation between classification score and localization precision. We also adopt the mixed-matching strategy, to facilitate DETR-based detectors with faster training convergence while keeping an end-to-end scheme. Moreover, to overcome the dramatic decrease in sample quality induced by the sparsity of queries, we introduce a prime sample weighting mechanism to suppress the interference of unimportant samples. Extensive experiments are conducted with very competitive results reported. In particular, it delivers a 46 (+3.8)% AP on the DAB-DETR baseline with the ResNet-50 backbone and reaches a new SOTA performance of 50.2% AP in the 1x setting on the COCO validation set when employing the strong baseline DINO. Our code is available at <https://github.com/FelixCaae/AlignDETR>.

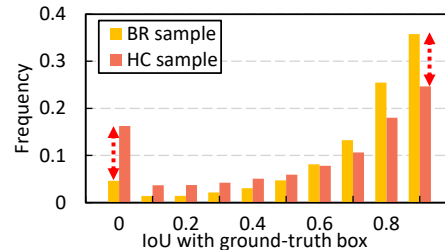
1. Introduction

Recently, transformer-based methods have gained significant attention in the community of object detection, due to the development of the DETR paradigm proposed by [2]. Different from the previous CNN-based detectors, DETR formulates this task as a set prediction problem and adopts learnable queries to represent each object in one-to-one cor-

*Work done during the internship at MEGVII Technology.



(a) Recalls of BR samples.



(b) IoU distributions of BR and HC samples.

Figure 1: (a) Recalls of the BR samples calculated on DINO with two losses, focal loss [21] and IA-BCE loss (ours). N denotes the number of ground truths and we calculate the recalls under different numbers of HC samples. (b) Frequency histogram of the IoU distributions of two types of samples. We use COCO *val.* as the test set for the two experiments.

respondence. Such unique correspondence derives from bipartite graph matching by means of label assignment during training. It bypasses the hand-crafted components such as non-maximum suppression (NMS) and anchor generation. With this simple and extensible pipeline, DETR shows great potential in a wide variety of areas, including 2D segmentation [4, 6, 17], 3D detection [34, 26, 24], *etc.*, in addition to 2D detection [31, 42].

During the past few years, the successors have advanced DETR in many ways. For instance, some methods attempt to incorporate local operators, such as ROI pooling [31] or deformable attention [42, 9], to increase the convergence

speed and reduce the computational cost; some methods indicate that those learnable queries can be improved through extra physical embeddings [25, 35, 23]; and some methods [16, 13, 3, 37] notice the defect of one-to-one matching and introduce more positive samples by adding training-only queries. Box refinement [42, 31, 37] is another helpful technique, which explicitly takes previous predictions as priors at the next stages.

Despite the recent progress in DETR-based detectors [2, 20, 42, 9, 37, 23], an underlying misalignment problem has been overlooked. This problem refers to the inconsistency of output predictions between the classification confidence and localization precision, *e.g.* a highly confident prediction with a relatively low intersection-over-union (IoU) score or vice versa [14, 19]. Ideally, the predictions with the highest classification scores (HC samples) also have the best-regressed bounding boxes (BR samples); however, it does not hold when the misalignment problem occurs, creating the risk of missing BR predictions and thus deteriorating the detection performance [14, 19].

Fig. 1a shows an empirical study on a strong baseline DINO [37], and the recall of BR samples by the well-trained model on the top- k confident outputs in an image is calculated, where a higher recall indicates that more BR samples are selected in final prediction. As we can see, only 45% and 48% BR samples are covered by HC samples with top- N and top- $2N$ scores, respectively, suggesting that more than half of the well-localized predictions have low confidence scores. In Fig. 1b, the frequency histogram of the HC and BR samples is plotted from 5,000 samples on COCO *val.* and a clear discrepancy between the two distributions is observed, revealing that even the highly-optimized model DINO [37] suffers from the misalignment problem.

In fact, this problem also appears in CNN-based detectors [14, 19, 38]. To address it, IoU-Net [14] proposes an individual IoU prediction branch and an IoU-guided NMS to align the classification confidence and regression precision. A number of alternatives [19, 38] introduce an IoU-aware loss or weight to integrate the IoU branch into the original classification branch and adopt a joint training strategy. These methods are specially designed for NMS-based detectors, but DETR implicitly selects samples by modeling query relations under the guidance of one-to-one matching without an explicit query selection step like NMS, making them less applicable to DETR [2, 42, 23, 37]. To the best of our knowledge, the misalignment problem still remains unexplored in the DETR series.

This paper investigates the solution to the misalignment problem in DETR. To this end, we propose a novel method, namely Align-DETR. It makes use of the standard binary cross-entropy (BCE) loss with an IoU-aware target on foreground samples, which we term the IA-BCE loss. For background samples, we still keep the focal loss [21] to conduct

hard-negative mining. The IA-BCE loss depends on a quality metric that combines the classification confidence and regression accuracy as a target and dynamically adjusts the target for foreground samples according to the quality metric, which smooths the training target and strengthens the correlation between classification and regression, hence increasing the chance for BR samples to be selected, as supported by the improved recall of the BR samples depicted in Fig. 1 (note that there is no change to the matching process).

Moreover, Align-DETR takes advantage of the many-to-one matching technique adopted in CNN-based object detectors [40, 11, 28] as well as recent DETR ones [16, 13, 3], which allows it to accelerate the training process. Despite this, another issue raises that assigning more positive samples tends to force some samples to be closely associated with the background. To overcome this difficulty, we then design a prime sample weighting scheme that downgrades the losses of the secondary positive samples.

Overall, Align-DETR offers a simple yet effective solution to the misalignment problem aforementioned, facilitating DETR in terms of better query selection and faster training speed. Equipped with a ResNet-50 [12] backbone and a DAB-DETR [23] baseline, our method achieves +3.8% AP gain under the schedule with 50 epochs. We also combine it with the strong baseline DINO [37] and establish a new SOTA performance with 50.2% AP in the $1\times$ setting on the COCO [22] validation set. To sum up, our contributions are three-fold. **First**, we are the first to spot the misalignment problem in the query selection mechanism of DETR and propose a metric, recall of BR samples, to evaluate it qualitatively. **Second**, we propose Align-DETR, which includes the IoU-aware BCE loss and the mixed-matching strategy, strengthened with prime sample weighting, as a strong baseline for the object detection task. **Last**, we conduct extensive experiments and ablations on COCO to validate the effectiveness of the proposed method with new SOTA results reported.

2. Related Work

2.1. End-to-end Object Detection

The pursuit of end-to-end object detection or segmentation dates back to several early efforts [27, 29, 30]. They rely on recurrent neural network (RNN) to remove duplicates or adopt a complex subnet to replace NMS. Recently, DETR [2] has established a set-prediction framework based on the transformer. Compared to previous work, DETR is rather simpler but still suffers from the downside of slow convergence with a number of subsequent DETR variants [42, 9, 8, 23, 16, 37] working on this issue. Some methods make improvements on the cross-attention in decoders [8, 25]. Deformable DETR [42] presents a deformable-attention module that only scans a small set of

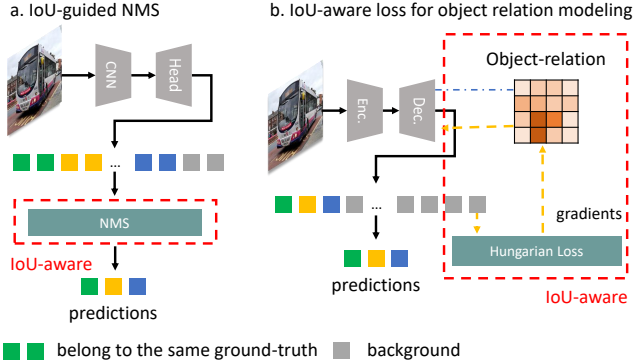


Figure 2: Comparison of the solutions to the misalignment problem. In CNN-based object detectors, the main efforts are made to guide the NMS [14] better selection. While ours IA-BCE focuses on improving the model’s relation modeling ability.

points near the reference point, while Sparse RCNN [31] makes use of ROI pooling to replace the attention module. Alternatively, others consider introducing prior knowledge into queries. Conditional-DETR [25] incorporates reference coordinates into the position embedding; SMCA [8] applies a modulated Gaussian bias; AnchorDETR [35] and DAB-DETR [23] turn to improving the learnable queries to eliminate the ambiguity of physical meanings; and Efficient DETR [36] conducts dense prediction in place of learnable queries. The recent DN-DETR [16] focuses on the unstable optimization process in one-to-one matching and relies on a denoising mechanism to stabilize the training, which is extended by DINO [37]. Despite the progress achieved, we observe that the problem of misalignment between classification confidence and regression accuracy widely exists in DETR-based detectors, which is still underexplored, leaving much room for improvement. In this work, we focus on this problem and aim at strengthening the correlation between the two sub-tasks.

A few recent studies have noticed limitations of one-to-one matching and have proposed many-to-one assigning strategies to ameliorate DETR regarding training efficiency. Group-DETR [3] accelerates the training process with multiple groups of samples and ground truths. H-DETR [13] introduces a hybrid branch mechanism to increase the training samples without ruining the end-to-end property. Thanks to their efforts, the DETR pipeline benefits from efficient training but at the cost of complexity and computation burden. For example, Group-DETR [3] and Hybrid-DETR [13] use 3300 (11 groups) and 1800 queries (5x in extra branch), respectively. In contrast, our proposed strategy does not introduce more queries and keeps the pipeline training efficient.

2.2. Label Assignment in Object Detection

As the CNN-based object detectors develop from the anchor-based framework to the anchor-free one, many works realize the importance of label assignment (which is previously hidden by anchor and IoU matching) during training. Some works [15, 11, 39] identify positive samples by measuring their dynamic prediction quality for each object.

Others [41, 19, 18, 10] learn the assignment in a soft way and achieve better alignment on prediction quality by incorporating IoU [19, 38] or a combination of IoU and confidence [41, 18, 10]. To make a clear comparison, we summarize some loss designs in Tab. 1.

Method	w_{pos}	w_{neg}	t
GFL [19]	$(s-t)^2 \cdot t$	$(s-t)^2 \cdot (1-t)$	IoU
VFL [38]	$t \cdot t$	$t \cdot (1-t)$	IoU
TOOD [7]	$(s-t)^2 \cdot t$	$(s-t)^2 \cdot (1-t)$	$f(IoU, s)$
MuSu [10]	$(s-t)^2 \cdot t$	$s^2 \cdot (1-t)^4$	$f(IoU, s)$
DW [18]	$f_{pos}(IoU, s)$	$P_{neg} \cdot I_{neg}$	-
IA-BCE (Ours)	t	$1-t$	$f(IoU, s)$

Table 1: Comparison with some related loss designs.

The misalignment problem in object detection has been addressed by various traditional solutions, such as incorporating an additional IoU-branch to fine-tune the confidence scores [14] or integrating the IoU prediction branch into classification losses [19]. Although they also design losses [19, 38], these approaches mainly improve the model’s performance through the NMS aspect as shown in Fig. 2.

In the contrast, this work solves the problem solely during training and makes no modifications to the post-processing. We illustrate the comparison in Fig. 2. We propose an IoU-aware BCE loss for DETR to better optimize the model. Notably, our method can also be seen as a soft-label assignment method.

3. Method

3.1. Motivation and Framework

First, DETR suffers from the problem of misalignment in output with inconsistent classification confidence and regression accuracy. This problem reduces the probability of BR samples being the resulting predictions and inevitably produce sub-optimal outputs (e.g. inaccurate bounding boxes but with confident classification scores). While the problem has been investigated in the previous literature [19, 38, 14], unfortunately, all the methods are either over-complicated in the loss design or not well-suited to DETR, which motivates us to design a proper solution dedicated to DETR. **Second**, DETR also suffers from slow

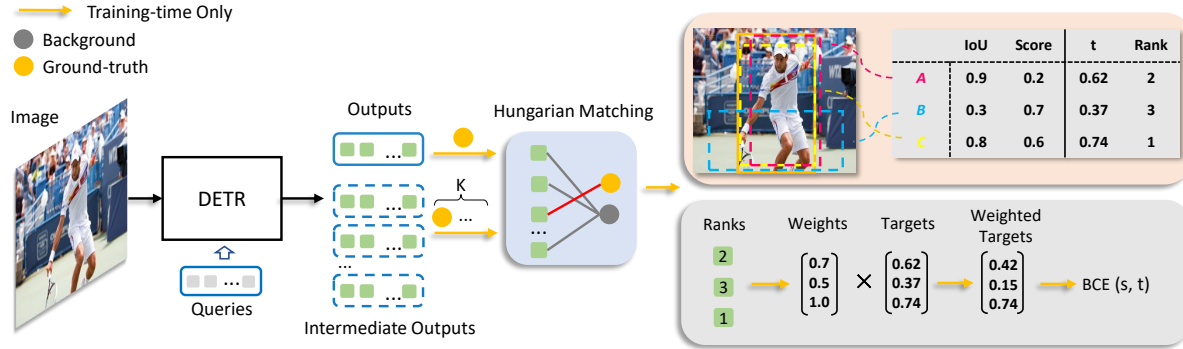


Figure 3: The architecture overview of the proposed approach Align-DETR. It mainly consists of two parts, matching and loss computation. One-to-one matching is applied on the output layer to remove duplicated predictions. And many-to-one matching is applied on the intermediate layers to accelerate training. After the matching, predictions are sent to an evaluation process to get their quality and relative ranks (the colored area). These results are then transformed into the targets for computing BCE loss (the gray area).

convergence. A common practice [33, 40, 3, 13] is applying a many-to-one matching strategy and one-to-one matching in different branches to maintain the property of end-to-end prediction. Differently, the other line of works [13, 36] apply the strategy at shallow decoder layers while keeping one-to-one matching at top layers. We choose to follow the second line as described in Sec. 3.4 since it introduces a minimal modification to the original pipeline with negligible extra computational burdens. Moreover, we find that the sparsity of queries leads to a problem in many-to-one label assignment. The increased positive samples in matching occasionally involve samples that are similar to the background (with poor quality). To address this issue, we propose a prime sample weighting strategy to configure the training target properly.

We illustrate our framework in Fig. 3 and introduce the detailed implementations in the following sections.

3.2. Preliminaries

The original DETR [2] framework consists of three main components: a CNN-backbone, an encoder-decoder transformer [32], and a prediction head. The backbone processes the input image first, and the resulting feature is flattened into a series of tokens $X = \{x_1, x_2, \dots, x_m\}$. Then the transformer extracts information from X with a group of learnable queries $Q = \{q_1, q_2, \dots, q_n\}$ as containers. At last, the updated queries are transformed into predictions $P = \{p_1, p_2, \dots, p_n\}$ through the prediction head. In most cases, m is much less than n , making DETR a sparse object detection pipeline.

DETR adopts the one-to-one label assignment on all layers to help eliminate redundant predictions. Given the ground truth (GT) $G = \{g_0, g_1, \dots, g_n\}$, which is padded with background tokens to the same size as predictions, the one-to-one label assignment finds a minimum weighted bi-

partite graph matching $\sigma \in \mathcal{S}$ between G and P as :

$$\sigma = \operatorname{argmin}_{\sigma \in \mathcal{S}} \sum_i^n \mathcal{L}_{match}(p_{\sigma(i)}, g_i), \quad (1)$$

$$\mathcal{L}_{match} = \mathcal{C}_{cls} + \mathcal{C}_{reg}, \quad (2)$$

where n is the number of predictions, \mathcal{S} is the set of all permutations and \mathcal{L}_{match} is a pair-wise matching cost that combines classification cost \mathcal{C}_{cls} and regression cost \mathcal{C}_{reg} .

DETR uses Hungarian loss \mathcal{L}_{o2o} as the training target defined as:

$$\mathcal{L}_{o2o} = \frac{1}{N_{gt}} \sum_i^n \lambda_{cls} \mathcal{L}_{cls} + \lambda_{reg} \mathcal{L}_{reg}, \quad (3)$$

where N_{gt} is the number of ground-truth objects, \mathcal{L}_{cls} is classification loss and \mathcal{L}_{reg} is regression loss. λ_{cls} and λ_{reg} are loss balance terms.

3.3. Iou-aware Classification Loss

Recall that DETR adopts a different mechanism to remove redundant predictions compared to CNN-based object detectors. In the decoder's self-attention modules, the final output is determined through the communication among all the queries, guided by the one-to-one matching as shown in Eq. 1. Additionally, it simply sums the classification cost and regression cost as individual metrics before matching in Eq. 2. This design expects the best samples to be matched in terms of regression and classification.

However, the original matching process ignores the misalignment between the classification score and regression accuracy and thus is incapable of ensuring that the BR samples have a high overlap with HC samples.

Inspired by previous works [19, 38, 14], we use a simple BCE loss with IoU as targets to align these two scores.

First, we define t as the weighted geometric average of the confidence score s and the IoU score (with ground-truth) u , similar to [10, 7]:

$$t = s^\alpha \cdot u^{(1-\alpha)}, \quad (4)$$

where α is a hyper-parameter that controls the proportion of each term, and we empirically find $\alpha = 0.25$ leads to the good results. The IoU score term in Eq. 4 takes the main role of guiding the model to build a strong relation between IoU accuracy and classification scores. Let $\alpha = 0$, $t = u$, and the loss target is fully IoU-dependant; let $\alpha = 1$, $t = s$ and the loss target is s , thus no training signals would be applied to s . In practice, we set α between 0 and 1 to strike a balance between the amount of guidance and training stability. We design an asymmetric classification loss, which assigns different weights to the foreground samples and background samples:

$$\mathcal{L}_{cls} = \sum_i^{N_{pos}} BCE(s_i, t_i) + \sum_j^{N_{neg}} s_j^2 BCE(s_j, 0), \quad (5)$$

where s is the predicted confidence score and t is the proposed metric that absorbs the IoU score. For foreground samples, we do not use the focal loss term to suppress ‘‘easy’’ positive samples, since positive samples in DETR are relatively rare, and we want to keep their influence [38]. For background samples, the focal loss weight s_j^2 is still kept to do the hard negative mining.

A detailed comparison between our method (IA-BCE) and other losses designed for the misalignment problem can be seen in Tab. 1. Different from previous solutions, such as MuSu [10], which have complicated forms, our loss design is much simpler, continuing the simplicity property of DETR.

3.4. Mixed Matching Strategy

Based on the consensus among the previous studies [37, 16, 13, 3, 33] that pure one-to-one label assignment is inefficient in training, we propose a mixed-matching strategy that utilizes many-to-one matching at shallow decoder layers and one-to-one matching at the top layer. As a result, more positive samples can participate in training, leading to faster convergence of the transformer structure.

First, we copy GT set G by k times to get G' for each intermediate layer and then input these new GT to the criterion. Then, in the matching process, one GT is assigned to k predictions, resulting in a total number of $(L - 1) \times (k - 1)$ auxiliary positive samples plus L original positive ones for each GT, where L is the number of decoder layers.

Though our mixed training strategy is motivated by the hybrid layer matching in H-DETR [13], we differ it in two ways: (a) H-DETR uses an increased number of augmented queries while we keep the query number unchanged for

computation efficiency; (b) H-DETR applies many-to-one matching at only a part of intermediate layers and introduce hand-craft designs while we apply it at all decoder layers but the last one.

In addition, our study in Section 4.3.3 reveals that assigning more positive samples does not necessarily result in greater benefits. We attribute this to the sparsity of queries, which leads to a dramatic decrease in sample quality as the ranks increased. This makes low-ranking positive samples similar to background [41, 37], which interferes with the learning of decision boundary. In this work, we calculate w_i of positive samples based on their ranks r_i sorted by t_i in a group (all samples belong to one GT), expressed as $w_i = exp(-r_i/\tau)$ where τ is the temperature controlling the sharpness. Then the classification loss is rewritten as:

$$\mathcal{L}_{cls} = \sum_i^{N_{pos}} BCE(s_i, w_i t_i) + \sum_j^{N_{neg}} s_j^2 BCE(s_j, 0), \quad (6)$$

where t_i is down-weighted by the w_i factor, and it produces a weaker target for secondary samples. We term this trick prime sample weighting. To be consistent, regression losses are also down-weighted by w_i as:

$$\mathcal{L}_{reg} = \sum_i^{N_{pos}} w_i l_{reg}(\hat{b}_i, b_i), \quad (7)$$

where $l_{reg}(\hat{b}_i, b_i)$ is the regression loss function applied on predicted bounding box \hat{b}_i and GT bounding box b_i .

Our final loss form is defined as:

$$\mathcal{L} = \sum_{l=1}^{L-1} \mathcal{L}_{m2o}(P_l, G') + \mathcal{L}_{o2o}(P_L, G), \quad (8)$$

where L is the number of decoder layers, P_l is the predictions of l th layer and \mathcal{L}_{m2o} has the same form as \mathcal{L}_{o2o} except that it receives an augmented version of G .

In summary, the Align-DETR introduces an IoU-aware BCE loss (IA-BCE) to solve the misalignment issue for higher precision on localization of DETR. It also extends the matching from pure one-to-one to many-to-one to accelerate the training. To overcome the sparsity of sample distribution, we introduce a prime sample weighting mechanism to suppress the weights of relatively unimportant samples.

4. Experiments

4.1. Setup

Datasets We conduct all our experiments on MS-COCO 2017 [22] Detection Track and report our results with the mean average precision (mAP) metric on the validation dataset.

Model	#epochs	AP	AP ₅₀	AP ₇₅	AP _S	AP _M	AP _L	Params	GFLOPS
DETR-R50 [2]	500	42.0	62.4	44.2	20.5	45.8	61.1	41M	86
Anchor DETR-R50 [35]	50	42.1	63.1	44.9	22.3	46.2	60.0	39M	--
Conditional DETR-R50 [25]	50	40.9	61.8	43.3	20.8	44.6	59.2	44M	90
DAB-DETR-R50 [23]	50	42.2	63.1	44.7	21.5	45.7	60.3	44M	94
DN-DETR-R50 [16]	50	44.1	64.4	46.7	22.9	48.0	63.4	44M	94
Align-DETR-R50	50	<u>46.0</u>	64.9	49.5	25.2	50.5	64.7	42M	94
DETR-R101 [2]	500	43.5	63.8	46.4	21.9	48.0	61.8	60M	152
Anchor DETR-R101 [35]	50	43.5	64.3	46.6	23.2	47.7	61.4	58M	--
Conditional DETR-R101 [25]	50	42.8	63.7	46.0	21.7	46.6	60.9	63M	156
DAB-DETR-R101 [23]	50	43.5	63.9	46.6	23.6	47.3	61.5	63M	174
DN-DETR-R101 [16]	50	45.2	65.5	48.3	24.1	49.1	65.1	63M	174
Align-DETR-R101	50	<u>46.9</u>	65.5	50.9	25.6	51.9	66	61M	174
DETR-DC5-R50 [2]	500	43.3	63.1	45.9	22.5	47.3	61.1	41M	187
Anchor DETR-DC5-R50 [35]	50	44.2	64.7	47.5	24.7	48.2	60.6	39M	151
Conditional DETR-DC5-R50 [25]	50	43.8	64.4	46.7	24.0	47.6	60.7	44M	195
DAB-DETR-DC5-R50 [23]	50	44.5	65.1	47.7	25.3	48.2	62.3	44M	202
DN-DETR-DC5-R50 [16]	50	46.3	66.4	49.7	26.7	50.0	64.3	44M	202
Align-DETR-DC5-R50	50	<u>48.3</u>	66.7	52.5	29.7	52.8	65.9	42M	200
DETR-DC5-R101 [2]	500	44.9	64.7	47.7	23.7	49.5	62.3	60M	253
Anchor DETR-DC5-R101 [35]	50	45.1	65.7	48.8	25.8	49.4	61.6	58M	--
Conditional DETR-DC5-R101 [25]	50	45.0	65.5	48.4	26.1	48.9	62.8	63M	262
DAB-DETR-DC5-R101 [23]	50	45.8	65.9	49.3	27.0	49.8	63.8	63M	282
DN-DETR-DC5-R101 [16]	50	47.3	67.5	50.8	28.6	51.5	65.0	63M	282
Align-DETR-DC5-R101	50	<u>49.3</u>	67.4	53.7	30.6	54.3	66.4	61M	280

Table 2: Results of our Align-DETR using DAB-DETR [23] as the baseline and other models. All models here use 300 queries except for DETR which uses 100 queries.

Model	#epochs	# queries	AP	AP ₅₀	AP ₇₅	AP _S	AP _M	AP _L	Params	GFLOPS
Faster RCNN-FPN [28]	108	--	42.0	62.1	45.5	26.6	45.5	53.4	42M	180
SMCA [8]	50	300	43.7	63.6	47.2	24.2	47.0	60.4	40M	--
Deformable DETR [42]	50	300	45.4	64.7	49.0	26.8	48.3	61.7	40M	235
DN-DETR [16]	12	300	43.4	61.9	47.2	24.8	46.8	59.4	48M	195
DAB-Deformable-DETR [23]	50	300	46.9	66.0	50.8	30.1	50.4	62.5	40M	173
DN-Deformable-DETR [16]	50	300	48.6	67.4	52.7	31.0	52.0	63.7	47M	23
DINO [37]	12	900	49.0	66.6	53.5	32.0	52.3	63	47M	279
DINO [37]	24	900	50.4	68.3	54.8	33.3	53.7	64.8	47M	279
GROUP-DETR [3]	12	2700	49.8	--	--	32.4	53.0	64.2	47M	--
H-Deformable-DETR [13]	12	1800	48.7	66.4	52.9	31.2	51.5	63.5	--	234
Align-DETR	12	900	<u>50.2</u>	67.8	54.4	32.9	53.3	65.0	47M	279
Align-DETR	24	900	<u>51.3</u>	68.2	56.1	35.5	55.1	65.6	47M	279

Table 3: Results of our Align-DETR using DINO [37] as the baseline and other methods, including CNN-based detectors and DETR-based detectors on COCO val. Align-DETR adopts a denoising mechanism and uses 100 cdn group [37].

Implementation details We use DAB-DETR [23] and DINO [37] as our baseline methods. The DAB-DETR baseline employs a standard transformer architecture that takes single-scale features as inputs. The DINO baseline adopts deformable-transformer [42] and multi-scale features as inputs. Our hyperparameters are set as $k = 3$, $\alpha = 0.25$, and $\tau = 1.5$. To optimize the models, we set the initial learning rate to 1×10^{-4} and decay it by multiplying 0.1 for back-

bone learning. We use AdamW with 1×10^{-4} weight decay as the optimizer and set 16 as batch size for all our experiments. To build our code, we use the open-source library detrex [5], along with their other default hyper-parameter settings.

To ensure a fair comparison, we separate single-scale methods and multi-scale methods for different groups. For comparing with single-scale DETR-variants, we train the

Method	AP	AP ₅₀	AP ₇₅
baseline (Focal loss)	49.0	66.0	53.5
w/ IoU branch* [14]	49.0	66.0	54.0
w/ IoU branch [14]	49.2	66.3	53.5
w/ QFL ($\gamma = 2$) [19]	47.6	64.3	51.8
w/ QFL ($\gamma = 1$) [19]	48.6	65.7	53.5
w/ VFL [38]	48.7	67.0	52.3
w/ IA-BCE (Ours)	<u>50.0</u>	<u>67.8</u>	<u>54.4</u>

Table 4: Comparison with other methods on the misalignment problem on COCO val. * represents no score fusing is performed. For the score fusing step, we set the weight factor of the IoU score to 0.3 for best results.

Align-DETR based on DAB-DETR [23] by 50 epochs and decay the learning rate by multiplying 0.1 at the 40th epoch. For comparison with multi-scale object detectors, we train Align-DETR based on DINO [37] for 1x and 2x schedules.

4.2. Main Results

4.2.1 Comparison with Single-scale Methods

Using the DAB-DETR [23] as the baseline, we conduct a series of experiments on different CNN backbones, including ResNet-50 (R50), ResNet-101 (R101), ResNet-50-DC5 (DC5-R50) and ResNet-101-DC5 (DC5-R101) to validate the effectiveness of our proposed Align-DETR. Our method is mainly compared with other competitive DETR variants, including our baseline DAB-DETR [23].

The results are summarized in Tab. 2. Our method Align-DETR surpasses the baseline by a large margin, *e.g.* Align-DETR has a 3.8% AP improvement on R50. In the reported results, DN-DETR shows strong competence, and even so, Align-DETR leads DN-DETR by 1~2% AP across several backbone settings. These improvements are mainly in the high IoU-threshold metric like AP₇₅ which supports our assumption that misalignment is a critical issue that downgrades the localization precision of DETR.

4.2.2 Comparison with Multi-scale Methods

We conduct experiments using DINO [37] as the baseline, which adopts the deformable-transformer as the backbone. DINO uses tricks such as CDN, look forward-twice, and bounding box refinement for better performance. We follow DINO’s approach and adopt its tricks. Regarding to backbone, we use an R-50 backbone with 4-scale features (P3, P4, P5, and P6) as input.

The results are presented in Tab. 3. Despite the highly optimized structure of DINO [37], our method still outperforms it by 1.2% and 0.9% AP in 1x and 2x schedules, respectively. This indicates that even the advanced DETR-variant can be affected by the misalignment problem. Then we compare Align-DETR to two recent state-

of-the-art methods, Group-DETR [3] and H-DETR [13], and find that Align-DETR achieves higher AP while using fewer queries, demonstrating its superior computational efficiency. It is worth noting that Align-DETR also outperforms other competitors such as SMCA [8], Faster RCNN-FPN [28], Deformable-DETR [42] with much less training schedule. These results suggest that Align-DETR is a highly effective and efficient method for object detection tasks.

IA-BCE	Mixed Matching	AP	AP ₅₀	AP ₇₅
✗	✗	49.0	66.0	53.5
✓	✗	50.0	67.8	54.2
✗	✓	49.1	67.5	53.4
✓	✓	<u>50.2</u>	<u>67.8</u>	<u>54.4</u>

Table 5: Ablation study of Align-DETR on each component in terms of AP on COCO val. The results demonstrate the effectiveness of our proposed component.

4.2.3 Comparison with Related Methods

In addition to comparison with state-of-the-art DETR-variants, we also implement methods like Quality Focal Loss (QFL) [19], and Varifocal Loss (VFL) [38] on DINO [37], and the results are presented in Tab. 4. Interestingly, we find that the IoU-branch brings limited improvement to the performance. We speculate that this may be due to the fact that the duplicate removal process in DETR is performed in the self-attention module through relation modeling. As a result, multiplying the IoU score with the confidence score only slightly changes the order of predictions and improves the ranking result in AP computation [1]. QFL [19] also performs poorly in our experiments and we assume their loss shapes are over-smoothed due to the focal loss term. Notably, we observe that decreasing the value of γ led to an improvement in performance. These findings support our hypothesis that DETR’s positive samples are rare and are not be suppressed too much. Compared to the most related method, VFL [38], our approach outperforms it in terms of average precision. VFL also deprecates the focal loss term, but our simpler design provides positive samples with stronger gradients, particularly when t is small during the early training stage. This is likely a contributing factor to the superior performance of our method.

4.3. Ablation Study

We conduct a series of ablation studies to validate the effectiveness of the components. All experiments here use an R50 backbone and a schedule of standard 1x training schedule.

α	0	0.25	0.5	0.75
AP	50.0	<u>50.2</u>	49.2	47.6

(a) Ablation studies on α

k	1	2	3	4
AP	50.0	50.1	<u>50.2</u>	50.2

(b) Ablation studies on k

τ	1.5	3	6	9
AP	<u>50.2</u>	50.1	50.0	49.7

(c) Ablation studies on τ

Table 6: Influence of hyper-paramters α , k and τ on our approach on COCO val.

4.3.1 Ablation Study on Components

We conduct a series of ablations on main components, including IA-BCE and Mixed Matching, to assess their effectiveness, and the results are summarized in Tab. 5. It is observed that both components contribute to the final performance, and the main contribution comes from IA-BCE loss. As for the mixed matching strategy, we speculate since DINO [37] already uses CDN group to support training, the gain may partially overlap with our method.

To further investigate the impact of the hyper-parameters we introduced, *i.e.* α , k and τ , we conduct sensitivity analysis by changing one variable and keeping other variables controlled. Our default values are $k = 3$, $\alpha = 0.25$, and $\tau = 1.5$. As shown in Tab. 6, α is has the greatest influence on the performance while τ and k have moderate effects. This sensitivity analysis supports our hypothesis that α should be kept small to prevent effective training signals from suppression.

Method	w/ IA-BCE	AP	AP ₅₀	AP ₇₅
H-Deformable-DETR [13]		48.7	66.4	52.9
H-Deformable-DETR [13]	✓	<u>49.3</u>	<u>67.2</u>	<u>53.7</u>

Table 7: Our IA-BCE applied on H-DETR on COCO val. All experiments are run with a 1x schedule.

4.3.2 Ablation Study on IoU-aware BCE Loss

To validate the generalizability of our approach, We apply our method IA-BCE on a strong competitor H-Deformable-DETR and achieve 0.6% AP improvement as shown in Tab. 7.

k	PS Weighting	AP	AP ₅₀	AP ₇₅
1		50.0	67.8	54.5
2		49.6	66.6	53.8
2	✓	50.1	67.5	54.2
3		49.7	66.7	53.9
3	✓	<u>50.2</u>	<u>67.8</u>	<u>54.4</u>

Table 8: Ablation study of prime sample weighting on COCO val. The first row represents the baseline where $k = 1$ and no prime sample weighting is applied.

4.3.3 Ablation Study on Prime Sample Weighting

We conduct ablation studies to validate the effectiveness of our proposed prime sample weighting. The results are represented in Tab. 8. After disabling prime sample weighting (PS Weighting), the performance drops by around 0.5% AP.

The comparison between the performance of models trained with and without prime sample weighting supports the effectiveness of this trick.

4.4. Visualization

To delve deeper into the improvement of our approach, we visualize and compare the confidence-IoU distribution of the outputs from the two models, DINO, and Align-DETR. The density map is transformed into a color map where a bright area represents a peak in distribution. As shown in Fig. 4, our approach performs better in aligning the two scores. To analyze the data quantitatively, we calculate the Pearson coefficients between the IoU and confidence, demonstrating the superiority of our method.

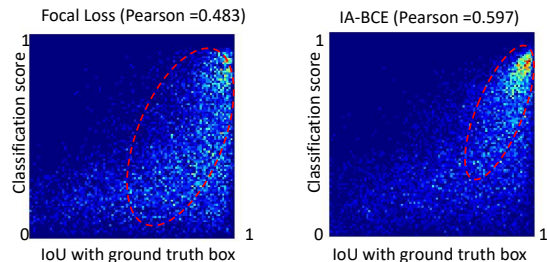


Figure 4: The hot-map figure visualizes the confidence and IoU’s distribution of matched samples in DINO and Align-DETR. The confidence of our approach is scaled to set the maximum to 1.

5. Conclusion

This paper examines a common problem, *i.e.* the misalignment problem, on DETR and observes its existence and importance of it. To address it, we propose a simple solution to this problem which is denoted as IA-BCE, which provides strong supervision on the correlation between classification score and localization precision. We also address the training inefficiency problem of DETR which is partially due to the one-to-one matching. To optimize the paradigm better, we propose a mixed matching strategy that applies many-to-one matching on intermediate predictions to provide richer training signals. To overcome the negative effect brought up by the poor label assignment, we pro-

pose prime sample weighting suppress the interference of unimportant samples. Competitive experimental results are achieved on the common COCO benchmark, demonstrating its superiority in effectiveness.

References

- [1] Yuhang Cao, Kai Chen, Chen Change Loy, and Dahua Lin. Prime sample attention in object detection. In *CVPR*, pages 11583–11591, 2020. 7
- [2] Nicolas Carion, Francisco Massa, Gabriel Synnaeve, Nicolas Usunier, Alexander Kirillov, and Sergey Zagoruyko. End-to-end object detection with transformers. In *ECCV*, 2020. 1, 2, 4, 6
- [3] Qiang Chen, Xiaokang Chen, Gang Zeng, and Jingdong Wang. Group detr: Fast training convergence with decoupled one-to-many label assignment. *arXiv preprint arXiv:2207.13085*, 2022. 2, 3, 4, 5, 6, 7
- [4] Bowen Cheng, Alex Schwing, and Alexander Kirillov. Pixel classification is not all you need for semantic segmentation. In *NeurIPS*, 2021. 1
- [5] detrex contributors. detrex: An research platform for transformer-based object detection algorithms. <https://github.com/IDEA-Research/detrex>, 2022. 6, 11
- [6] Bin Dong, Fangao Zeng, Tiancai Wang, Xiangyu Zhang, and Yichen Wei. Solq: Segmenting objects by learning queries. In *NeurIPS*, 2021. 1
- [7] Chengjian Feng, Yujie Zhong, Yu Gao, Matthew R Scott, and Weilin Huang. Toood: Task-aligned one-stage object detection. In *ICCV*, pages 3490–3499. IEEE Computer Society, 2021. 3, 5
- [8] Peng Gao, Minghang Zheng, Xiaogang Wang, Jifeng Dai, and Hongsheng Li. Fast convergence of detr with spatially modulated co-attention. In *ICCV*, 2021. 2, 3, 6, 7
- [9] Ziteng Gao, Limin Wang, Bing Han, and Sheng Guo. Adamixer: A fast-converging query-based object detector. In *CVPR*, 2022. 1, 2
- [10] Ziteng Gao, Limin Wang, and Gangshan Wu. Mutual supervision for dense object detection. In *CVPR*, pages 3641–3650, 2021. 3, 5
- [11] Zheng Ge, Songtao Liu, Zeming Li, Osamu Yoshie, and Jian Sun. Ota: Optimal transport assignment for object detection. In *CVPR*, 2021. 2, 3
- [12] Kaiming He, Xiangyu Zhang, Shaoqing Ren, and Jian Sun. Deep residual learning for image recognition. In *CVPR*, 2016. 2
- [13] Ding Jia, Yuhui Yuan, Haodi He, Xiaopei Wu, Haojun Yu, Weihong Lin, Lei Sun, Chao Zhang, and Han Hu. Detsrs with hybrid matching. *arXiv preprint arXiv:2207.13080*, 2022. 2, 3, 4, 5, 6, 7, 8
- [14] Borui Jiang, Ruixuan Luo, Jiayuan Mao, Tete Xiao, and Yunying Jiang. Acquisition of localization confidence for accurate object detection. In *ECCV*, pages 784–799, 2018. 2, 3, 4, 7
- [15] Kang Kim and Hee Seok Lee. Probabilistic anchor assignment with iou prediction for object detection. In *ECCV*, 2020. 3
- [16] Feng Li, Hao Zhang, Shilong Liu, Jian Guo, Lionel M Ni, and Lei Zhang. Dn-detr: Accelerate detr training by introducing query denoising. In *CVPR*, 2022. 2, 3, 5, 6
- [17] Feng Li, Hao Zhang, Shilong Liu, Lei Zhang, Lionel M Ni, Heung-Yeung Shum, et al. Mask dino: Towards a unified transformer-based framework for object detection and segmentation. *arXiv preprint arXiv:2206.02777*, 2022. 1
- [18] Shuai Li, Chenhang He, Ruihuang Li, and Lei Zhang. A dual weighting label assignment scheme for object detection. In *CVPR*, 2022. 3
- [19] Xiang Li, Wenhai Wang, Lijun Wu, Shuo Chen, Xiaolin Hu, Jun Li, Jinhui Tang, and Jian Yang. Generalized focal loss: Learning qualified and distributed bounding boxes for dense object detection. In *NeurIPS*, 2020. 2, 3, 4, 7
- [20] Junyu Lin, Xiaofeng Mao, Yuefeng Chen, Lei Xu, Yuan He, and Hui Xue. D²etr: Decoder-only detr with computationally efficient cross-scale attention. *arXiv preprint arXiv:2203.00860*, 2022. 2
- [21] Tsung-Yi Lin, Priya Goyal, Ross Girshick, Kaiming He, and Piotr Dollár. Focal loss for dense object detection. In *ICCV*, pages 2980–2988, 2017. 1, 2
- [22] Tsung-Yi Lin, Michael Maire, Serge Belongie, James Hays, Pietro Perona, Deva Ramanan, Piotr Dollár, and C Lawrence Zitnick. Microsoft coco: Common objects in context. In *ECCV*, 2014. 2, 5
- [23] Shilong Liu, Feng Li, Hao Zhang, Xiao Yang, Xianbiao Qi, Hang Su, Jun Zhu, and Lei Zhang. Dab-detr: Dynamic anchor boxes are better queries for detr. *arXiv preprint arXiv:2201.12329*, 2022. 2, 3, 6, 7
- [24] Yingfei Liu, Tiancai Wang, Xiangyu Zhang, and Jian Sun. Petr: Position embedding transformation for multi-view 3d object detection. *arXiv preprint arXiv:2203.05625*, 2022. 1
- [25] Depu Meng, Xiaokang Chen, Zejia Fan, Gang Zeng, Houqiang Li, Yuhui Yuan, Lei Sun, and Jingdong Wang. Conditional detr for fast training convergence. In *ICCV*, 2021. 2, 3, 6
- [26] Ishan Misra, Rohit Girdhar, and Armand Joulin. An end-to-end transformer model for 3d object detection. In *ICCV*, 2021. 1
- [27] Mengye Ren and Richard S Zemel. End-to-end instance segmentation with recurrent attention. In *CVPR*, 2017. 2
- [28] Shaoqing Ren, Kaiming He, Ross Girshick, and Jian Sun. Faster r-cnn: Towards real-time object detection with region proposal networks. In *NeurIPS*, 2015. 2, 6, 7
- [29] Amaia Salvador, Miriam Bellver, Victor Campos, Manel Baradad, Ferran Marques, Jordi Torres, and Xavier Giro-i Nieto. Recurrent neural networks for semantic instance segmentation. *arXiv preprint arXiv:1712.00617*, 2017. 2
- [30] Russell Stewart, Mykhaylo Andriluka, and Andrew Y Ng. End-to-end people detection in crowded scenes. In *CVPR*, 2016. 2
- [31] Peize Sun, Rufeng Zhang, Yi Jiang, Tao Kong, Chenfeng Xu, Wei Zhan, Masayoshi Tomizuka, Lei Li, Zehuan Yuan, Changhu Wang, et al. Sparse r-cnn: End-to-end object detection with learnable proposals. In *CVPR*, 2021. 1, 2, 3
- [32] Ashish Vaswani, Noam Shazeer, Niki Parmar, Jakob Uszkoreit, Llion Jones, Aidan N Gomez, Łukasz Kaiser, and Illia Polosukhin. Attention is all you need. In *NeurIPS*, 2017. 4

- [33] Jianfeng Wang, Lin Song, Zeming Li, Hongbin Sun, Jian Sun, and Nanning Zheng. End-to-end object detection with fully convolutional network. In *CVPR*, 2021. 4, 5
- [34] Yue Wang, Vitor Campagnolo Guizilini, Tianyuan Zhang, Yilun Wang, Hang Zhao, and Justin Solomon. Detr3d: 3d object detection from multi-view images via 3d-to-2d queries. In *CoRL*, 2022. 1
- [35] Yingming Wang, Xiangyu Zhang, Tong Yang, and Jian Sun. Anchor detr: Query design for transformer-based detector. In *AAAI*, 2022. 2, 3, 6
- [36] Zhuyu Yao, Jiangbo Ai, Boxun Li, and Chi Zhang. Efficient detr: improving end-to-end object detector with dense prior. *arXiv preprint arXiv:2104.01318*, 2021. 3, 4
- [37] Hao Zhang, Feng Li, Shilong Liu, Lei Zhang, Hang Su, Jun Zhu, Lionel M Ni, and Heung-Yeung Shum. Dino: Detr with improved denoising anchor boxes for end-to-end object detection. *arXiv preprint arXiv:2203.03605*, 2022. 2, 3, 5, 6, 7, 8, 11, 12
- [38] Haoyang Zhang, Ying Wang, Feras Dayoub, and Niko Sunderhauf. Varifocalnet: An iou-aware dense object detector. In *CVPR*, pages 8514–8523, 2021. 2, 3, 4, 5, 7
- [39] Shifeng Zhang, Cheng Chi, Yongqiang Yao, Zhen Lei, and Stan Z Li. Bridging the gap between anchor-based and anchor-free detection via adaptive training sample selection. In *CVPR*, 2020. 3
- [40] Qiang Zhou, Chaohui Yu, Chunhua Shen, Zhibin Wang, and Hao Li. Object detection made simpler by eliminating heuristic nms. *arXiv preprint arXiv:2101.11782*, 2021. 2, 4
- [41] Benjin Zhu, Jianfeng Wang, Zhengkai Jiang, Fuhang Zong, Songtao Liu, Zeming Li, and Jian Sun. Autoassign: Differentiable label assignment for dense object detection. *arXiv preprint arXiv:2007.03496*, 2020. 3, 5
- [42] Xizhou Zhu, Weijie Su, Lewei Lu, Bin Li, Xiaogang Wang, and Jifeng Dai. Deformable detr: Deformable transformers for end-to-end object detection. *arXiv preprint arXiv:2010.04159*, 2020. 1, 2, 6, 7

Appendix for Align-DETR

Algorithm 1 Pseudo-code of loss computing in Align-DETR in a Pytorch-like style.

```

# P: classification output (activated)
# B: regression output (activated)
# G: ground truth
# alpha: balancing factor in quality
# tau: temperature in prime sample weighting
# gamma: focal loss gamma
# k: the number of GT to be copied
# N_gt: the number of ground truth
#1. compute the Hungarian matching result
pos_ind, gt_ind = match(P, B, G, k)

#2. compute the matched predictions' IoU scores
IoU = box_IoU(B[pos_ind], G[gt_ind])

#3. compute the matched prediction's quality
quality = P[pos_ind] ** alpha * IoU ** (1-alpha)
quality = quality.detach()

#4. sort the quality locally and get each item's rank
rank = local_sort(quality, k, descending=True)

#5. get the prime sample weighting factor
w_p = exp(-rank/tau)

#6. initialize weights for BCE loss
pos_w = zeros_like(P)
pos_w[pos_ind] = w_p * quality
neg_w = P ** gamma
neg_w[pos_ind] = 1 - w_p * quality

#7. compute BCE loss
loss_cls = (-pos_w * P.log() - neg_w * (1-P).log()).sum() / N_gt

#8. compute regression loss
loss_reg = (w_p * reg_loss(P[pos_ind], G[gt_ind])).sum() / N_gt

```

A. Pseudo-code

We present the implementation of our Align-DETR with PyTorch-style pseudo-code in Alg. 1. As can be seen, our method is easy to be implemented.

B. Configuration

We list all the common hyper-parameters used by our method Align-DETR in Tab. A. Most of the hyper-parameters follow DINO [37] and detrex [5].

C. Ablation study on IA-BCE loss

We conduct ablation studies on the design of our loss functions and test different variants of IA-BCE. All loss functions adopt a general form of binary cross entropy loss as $\mathcal{L}_{cls} = w_{pos} \cdot \ln(s) - w_{neg} \cdot \ln(1-s)$. The results are shown in Tab. B. We attempt to simplify our loss functions by trying simpler variants in the second row and third row, but the performance dropped by 2.5% AP and 2.0% AP, respectively. This suggests that our loss function can not be further simplified. In the third and fourth rows, we try some

Item	Value
features	(“res3“, “res4“, “res5“)
freeze bn	Yes
position embedding temperature	10000
embed_dim	256
num_heads	8
feedforward_dim	2048
dropout	0
num_layers	6
post_norm	False
num_classes	80
num_queries	900
cost_class	2.0
cost_bbox	5.0
cost_giou	2.0
cost_class_type	focal loss
cost_alpha	0.25
cost_gamma	2.0
loss_class	1.0
loss_bbox	5.0
loss_giou	2.0
loss_class_dn	1.0
loss_bbox_dn	5.0
loss_giou_dn	2.0
dn_number	100
label_noise_ratio	0.5
box_noise_scale	1.0
k	3
loss_gamma	2.0
loss_tau	1.5
loss_alpha	0.25

Table A: Configuration of Align-DETR with DINO baseline (mAP 50.2%). **Red**: our introduced hyper-parameters.

w_{pos}	w_{neg}	AP	AP ₅₀	AP ₇₅
$(1-s)^2$	0	49.0	66.6	53.5
1	0	47.5	67.6	51.1
t	0	48.0	67.6	51.8
$(t-s)^2$	$(t-s)^2$	49.6	67.1	54.0
$(t-s)^2$	$(1-t)s^2$	49.8	66.2	<u>54.5</u>
t	$1-t$	<u>50.0</u>	<u>67.8</u>	<u>54.5</u>

Table B: Comparison of some variants of our IA-BCE on COCO val. The baseline (focal loss) is shown in the first row. Our IA-BCE is shown in the last row. We use $\alpha = 0.25$ to compute t .

complex variants but achieve slightly lower results, which validates the effectiveness of our final loss.

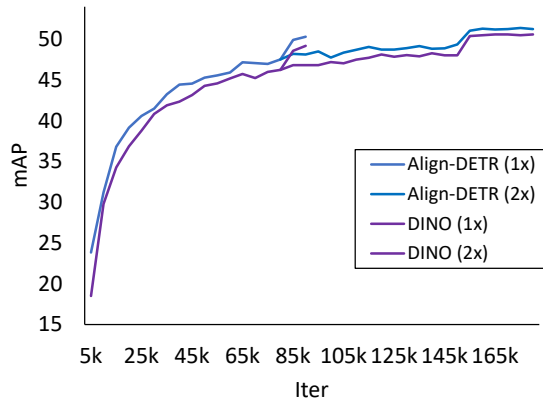


Figure A: The training curves of our Align-DETR, and DINO [37] in 1x and 2x schedules on COCO val.

D. Training curves of Align-DETR

We plot the training curves of our method and compare it with those of DINO [37] in 1x and 2x schedules. The result is presented in Fig. A. As shown in the figure, our method achieves higher results throughout the entire training process and benefits from faster convergence.

E. Visualization of prediction results

We randomly select some samples from the COCO validation set and plot their prediction results by Align-DETR, as shown in Fig. B.

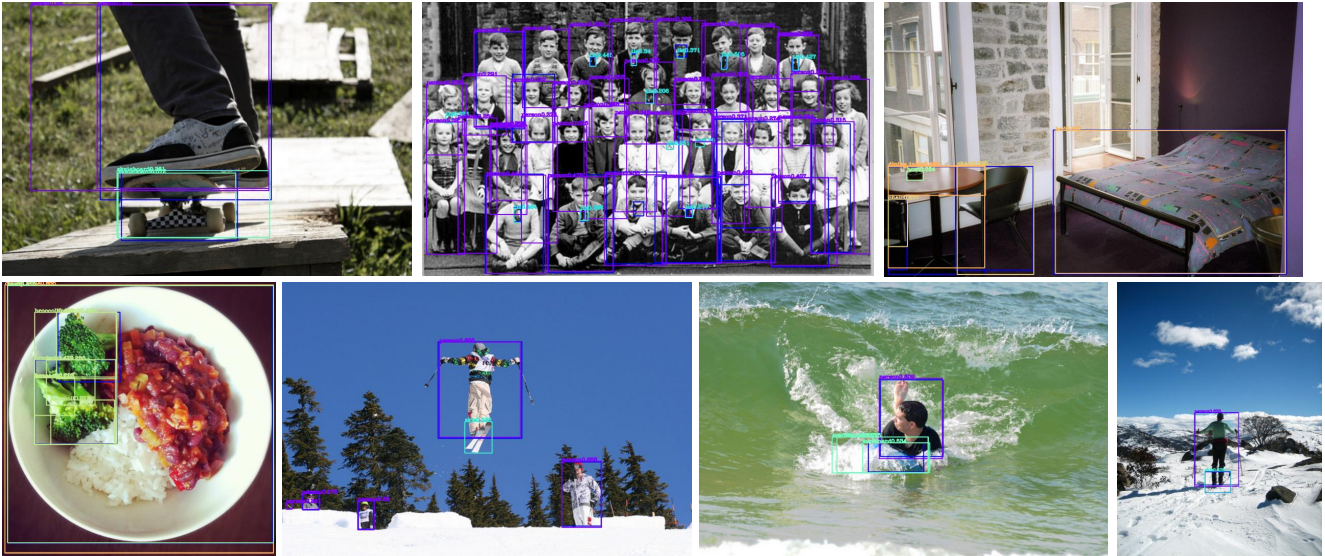


Figure B: Visualization of some predictions randomly selected from COCO val. **Blue** boxes are ground truths and the confidence threshold is set 0.2.